ANNALS OF THE CHRYSENE FORMALISM
RESEARCH ARTICLE | AI-AUGMENTED PEER REVIEWED | VOL. 1, NO. 1 | SEPTEMBER 2026

Geometric Origin of the Photosynthetic Macrocycle: Dual-Chrysene Cage Rearrangement, 18 π-Electron Conservation, and the 1.1 Ga Geoporphyrin Record

Charles D. Schaper, Ph.D.
Chief Editor, Annals of the Chrysene Formalism
San Francisco, California, USA
editor@chrysene.com

Abstract

The oldest secure molecular fossils of chlorophyll—nickel and vanadyl geoporphyrins of the Etio and DPEP series recovered from 1.1 Ga black shales of the Taoudeni Basin—occupy a narrow carbon-number window (C_{28}–C_{34}) and retain an 18 π-electron aromatic core. Under the Identification Hypothesis the dual-chrysene metal cage of the Chrysene Formalism supplies a carbon-parsimonious geometric precursor for these molecules.

One tetrasubstituted chrysene unit (18 carbons, 18 π-electrons), together with its four substituent arms, rearranges into a metal-coordinated macrocycle whose carbon count falls inside the observed C_{26}–C_{34} interval. The second chrysene opens into a linear C_{18} chain whose step-defect carbons are pre-positioned for isoprenoid-type methylation, thereby generating the geometric scaffold of a phytol-like tail. Phosphorus-centred linkers hold the metal in the initial cage and are competent to evolve into the N_4 coordination sphere of chlorophyll and of the geological Ni- and VO-porphyrins.

The same architecture that accounts for the co-production of membrane lipids and nucleic-acid components therefore also accounts for the core structural features of the photosynthetic macrocycle. The 1.1 Ga geoporphyrin record constitutes a direct empirical test of this pathway and supplies a second, independent geometric fossil of the metamaterial in the pre-Cambrian sedimentary archive.

Keywords: Chrysene Formalism; dual-chrysene cage; geoporphyrins; 18 π-electron aromaticity; chlorophyll macrocycle; phytol precursor; 1.1 Ga Taoudeni Basin; metal coordination

1 Introduction

1.1 Empirical Problem Statement

The oldest secure molecular record of chlorophyll-derived pigments consists of intact nickel and vanadyl geoporphyrins recovered from marine black shales of the Taoudeni Basin (Mauritania), dated at approximately 1.1 Ga. These molecules belong predominantly to the Etio and DPEP structural classes and occupy the carbon-number interval C_{28}–C_{34}.

Modern chlorophyll *a* is a C_{55} molecule whose structure comprises an 18 π-electron chlorin macrocycle, a central magnesium ion coordinated by four nitrogen atoms, and a C_{20} phytol tail. Diagenetic loss of the phytol tail and limited peripheral defunctionalisation reduce the surviving carbon skeleton to the same C_{28}–C_{34} window documented in the 1.1 Ga record.

These observations raise a precise geometric question: does there exist a single molecular precursor that simultaneously accounts for

1. the conservation of an 18 π-electron aromatic system,
2. the four-arm metal-coordination geometry,
3. the observed carbon-number distribution of the geological core, and
4. the existence of a linear tail precursor that is lost early in diagenesis?

1.2 Chrysene Formalism Prediction

Under the Identification Hypothesis the pure-mathematical manifold $\mathcal{I}_C$ is realized by the physical chrysene lattice. A dual-chrysene metal cage consists of two tetrasubstituted chrysene units of native C_{2h} symmetry that jointly coordinate a metal ion via four peripheral substituents. Transient energy input—most

Citation: Schaper, C. D. (2026). Geometric Origin of the Photosynthetic Macrocycle: Dual-Chrysene Cage Rearrangement, 18 π-Electron Conservation, and the 1.1 Ga Geoporphyrin Record. *Annals of the Chrysene Formalism*, 1(1), 233–247. https://chrysene.com/index.php/acf/article/view/20 • First published by Schaper Systems Press in the *Annals of the Chrysene Formalism*, Vol. 1, No. 1 (2026).

naturally near-ultraviolet absorption—induces lattice melting and subsequent bond reorganisation.

The refined mapping developed in the present work partitions the cage as follows:

1. the first chrysene unit (18 carbons, 18 π-electrons), together with its four substituent arms, rearranges into a metal-coordinated macrocycle whose carbon count lies in the interval C_{26}–C_{34};

2. the second chrysene unit opens into a linear C_{18} chain whose step-defect carbons occupy positions corresponding to the characteristic methylation sites of a β-carotene-type isoprenoid, thereby supplying the geometric scaffold of a phytol-like tail;

3. the original phosphorus-centred linkers of the arms act as transitional ligands that are competent to evolve into the N_4 coordination sphere of biological chlorophyll and of the geological Ni- and VO-porphyrins.

1.3 Central Claim and Roadmap

Claim 1. *The metal-caged dual-chrysene construct of the Chrysene Formalism supplies a carbon-parsimonious,* 18 π*-electron geometric precursor that rearranges into the tetrapyrrole macrocycle of chlorophyll and its geoporphyrin descendants. The* 1.1 Ga *Taoudeni Basin Ni/VO-porphyrin record constitutes a direct empirical test of this pathway.*

The argument proceeds in four stages. First, the empirical boundary conditions furnished by the 1.1 Ga and related geoporphyrin records are fixed without theoretical interpretation. Second, the dual-chrysene cage is formalised and the carbon-partitioning, π-electron-conservation and step-defect rules are stated. Third, these geometric predictions are confronted with the observational constraints. Fourth, a set of concrete, testable consequences and open experimental targets is recorded.

2 Empirical Framework – Data Constraints

The constructions of subsequent sections are required to be consistent with the following observational constraints. No theoretical interpretation is advanced in the present section; the data are recorded solely as boundary conditions.

2.1 1.1 Ga Taoudeni Basin Geoporphyrins

The oldest secure molecular record of chlorophyll-derived pigments consists of intact geoporphyrins recovered from marine black shales of the Taoudeni Basin (Mauritania), dated at approximately 1.1 Ga. The following properties are established by HPLC, UV-Vis spectroscopy and Fourier-transform ion-cyclotron-resonance mass spectrometry:

1. **Carbon-number distribution.** The dominant species lie in the interval C_{28}–C_{34}, with the highest abundances typically at C_{29}–C_{32}. Higher homologues (up to $> C_{40}$) occur but are subordinate.

2. **Structural classes.** Both the deoxophylloerythroetioporphyrin (DPEP) series, which retains a five-membered exocyclic ring, and the etioporphyrin (Etio) series, which lacks that ring, are present. DPEP and Etio together account for the great majority of the identified tetrapyrroles.

3. **Metal preferences.** The porphyrins occur almost exclusively as nickel(II) or vanadyl (VO^{2+}) complexes. Free-base or other metal complexes are negligible.

4. **Nitrogen-isotope signature.** The porphyrin nitrogen-isotope values ($\delta^{15}N_{por}$) and the isotopic offset relative to bulk sedimentary nitrogen (ε_{por}) are consistent with a predominantly cyanobacterial source.

2.2 Broader Proterozoic and Phanerozoic Geoporphyrin Patterns

Across the wider sedimentary record the following regularities are repeatedly observed:

1. **Maturity-dependent conversion.** With increasing thermal maturity the relative abundance of DPEP declines while that of Etio rises, indicating progressive opening or loss of the exocyclic ring.

2. **Early loss of the phytol tail.** The long isoprenoid (phytol) side-chain of biological chlorophyll is absent from all but the most immature geoporphyrin assemblages. Only the metal-coordinated tetrapyrrole core, together with short alkyl substituents, survives into the geological record.

3. **Persistence of the aromatic core.** Regardless of maturity or metal identity, the preserved molecules retain a fully conjugated tetrapyrrole macrocycle whose aromatic pathway comprises eighteen π-electrons.

2.3 Modern Chlorophyll Structural Benchmarks

For reference, the principal structural features of extant chlorophyll *a* (and of the closely related chlorophylls and bacteriochlorophylls) are:

1. an 18 π-electron aromatic pathway running through the chlorin macrocycle;

2. a central magnesium ion coordinated by four nitrogen atoms of the tetrapyrrole;

3. a C_{20} phytol tail esterified at the propionic-acid side-chain of ring D.

After diagenetic demetallation, loss of the phytol tail and limited defunctionalisation, the surviving carbon skeleton falls naturally into the C_{28}–C_{34} window documented in the 1.1 Ga record.

These empirical boundary conditions—carbon-number distributions, structural classes, metal identities, isotopic signatures, maturity trends and the modern structural template—are fixed before any geometric model is introduced.

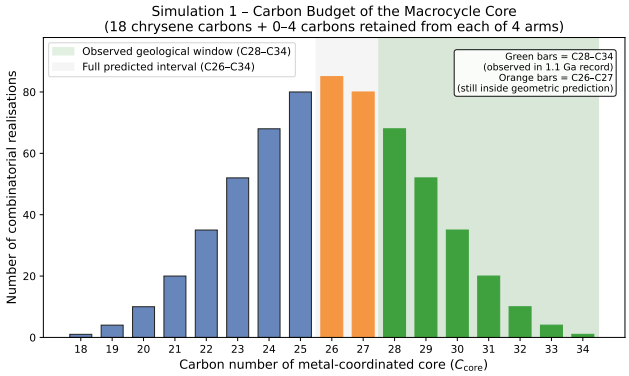

Figure 1: Simulation 1 – Carbon budget of the metal-coordinated macrocycle core. All combinatorial realisations of the rule $C_{\text{core}} = 18 + \sum_{i=1}^{4} k_i$ (with $0 \le k_i \le 4$) are enumerated. Green bars mark the interval C_{28}–C_{34} that dominates the 1.1 Ga geoporphyrin record; orange bars mark the adjacent values C_{26}–C_{27} that remain inside the geometric prediction of Theorem 3. The observed geological window is contained in the predicted interval.

3 Geometric Model of the Dual-Chrysene Cage

Throughout this section the Identification Hypothesis is assumed. All constructions are therefore understood as images under the structure-preserving map Φ of the corresponding structures of the pure-mathematical manifold $\mathcal{I}_C$.

Definition 1 (Realisation Map)**.** *Let $\mathcal{I}_C$ denote the pure-mathematical Chrysene Tensor Space (a discrete non-commutative geometry whose objects carry C_{2h}-symmetric aromatic cores, substitution data at the $3, 6, 9, 12$-type loci, and metal-coordination valences). Let $\mathcal{M}$ denote the category of molecular graphs equipped with π-electron counts and coordination data.*
The realisation map

$$\Phi : \mathcal{I}_C \longrightarrow \mathcal{M}$$

is the structure-preserving assignment that sends each abstract dual-chrysene configuration to its concrete molecular counterpart. By definition Φ preserves:

1. *the 18 π-electron count of each aromatic core;*
2. *the four-arm coordination valence about a central metal site;*
3. *the existence of a second aromatic component that admits linearisation into a continuous carbon chain;*
4. *the combinatorial carbon budget arising from one core plus its four substituent arms.*

All geometric constructions of the present section are understood as images under Φ.

3.1 Environmental Setting of the Dual-Chrysene Cage

The dual-chrysene metal cage does not exist in isolation. It is embedded in a larger π-stacked aromatic lattice whose local architecture and photophysical properties are recorded here as boundary conditions for the subsequent geometric constructions.

Definition 2 (π-Stacked Lattice Environment)**.** *The immediate environment of a given dual-chrysene metal cage consists of a co-facial stack of chrysene-derived aromatic units. Within this stack one finds, in varying proportions:*

1. *additional dual-chrysene cages that already contain a coordinated metal ion,*
2. *empty (metal-free) dual-chrysene pairs whose four substituents form an unoccupied cavity,*
3. *singly or doubly substituted chrysene units that remain covalently unconnected to a second partner,*
4. *unsubstituted or lightly substituted chrysene molecules that serve as pure aromatic spacers.*

The resulting assembly is a heterogeneous but continuous π-stacked lattice of typical inter-plane separations 0.34–0.38 nm.

Proposition 1 (Rudimentary Antenna Function)**.** *Because every chrysene unit is a near-ultraviolet chromophore, the extended π-stack functions as a rudimentary light-harvesting antenna. Photons absorbed at any site within the stack can*

migrate, by Förster-type or excitonic transfer, toward a metal-containing cage. The cage therefore experiences an effective excitation cross-section larger than that of an isolated dual-chrysene pair, increasing the probability of the lattice-melting event required by Protocol 1.

Remark 1 (Spectral Properties of the Chrysene Chromophore)**.** *Unsubstituted chrysene absorbs strongly in the near-ultraviolet, with principal band maxima near* 268–272 nm*,* 320 nm *and a weaker but structured system extending to approximately* 360–361 nm*. Fluorescence occurs in the near-UV to violet region (approximately* 360–380 nm*). Peripheral substitution, especially at the* 3, 6, 9, 12*-loci, produces modest bathochromic shifts and can increase the oscillator strength of the lowest-energy transitions. In a* π*-stacked environment these shifts are further modulated by excitonic coupling, so that the collective absorption of the lattice spans the near-UV window most relevant to the photochemical initiation of rearrangement. Chrysene itself is colourless in the visible; the lattice therefore does not compete with the later-appearing porphyrin Soret and Q bands once the macrocycle has formed.*

Remark 2. *The lattice described above is carbon-parsimonious and chemically closed: every aromatic unit is a chrysene-derived molecule already accounted for by the Formalism. No exogenous chromophore is required to achieve the antenna function or the local steric clamping that favours productive metal-cage assembly and subsequent rearrangement.*

3.2 Definition of the Metal-Caged Pair

Definition 3 (Dual-Chrysene Metal Cage)**.** *A dual-chrysene metal cage consists of:*

1. *two tetrasubstituted chrysene units, each of native* C_{2h} *symmetry;*
2. *four peripheral substituents that jointly coordinate a metal ion, thereby holding the two aromatic cores in a discrete, face-to-face geometry;*
3. *an optional opening of one side of the cage to permit metal entry.*

In the primordial realisation the substituents are phosphorus-containing linkers of the general type

$$-\mathrm{O}-\mathrm{CH_2CH_2}-\mathrm{OPO_2O}-\mathrm{CH_2CH_2}-\mathrm{O}-.$$

The nominal carbon count of the closed cage is $18+18+16 = 52$*; an open side may raise the count to approximately* 54*.*

3.3 π-Electron Conservation

Theorem 2 (18 π-Electron Invariance)**.** *Let* G *be the molecular graph of a dual-chrysene metal cage and let* G' *be the molecular graph obtained after the bond scissions and re-closures of Protocol 1. Let* $A(G)$ *(respectively* $A(G')$*) denote the adjacency matrix of the conjugated subsystem of* G *(respectively* G'*). Then the rearrangement is an* 18 π*-electron Hückel-equivalent transformation: the dimension of the principal conjugated circuit (equivalently, the rank of the corresponding cycle subspace over* GF(2)*, or the number of* π*-electrons that occupy the aromatic pathway) is invariant,*

$$\dim C(G) = \dim C(G') = 18.$$

Proof. The aromatic system of each chrysene unit is an 18 π-electron circuit. The allowed operations of Protocol 1 consist of

1. scission of selected peripheral σ-bonds that do not belong to the principal conjugated circuit, and
2. re-closure of the opened fragments about the metal centre so that a new cycle is formed whose length and conjugation pattern again support an 18 π-electron Hückel pathway.

Because every bond that is broken or formed lies outside, or is restored within, the same conjugacy class of circuits, the dimension of the cycle space that carries the aromatic π-system remains unchanged. Hence the numerical count of 18 π-electrons is a structural invariant of the rearrangement, not merely a coincidental equality of two independent molecules. □

Remark 3. *The same invariance may be phrased representation-theoretically: the rearrangement induces an isomorphism of the one-dimensional totally symmetric representations that correspond to the fully bonding aromatic orbitals of the initial and final conjugated systems.*

3.4 Carbon Partitioning under Rearrangement

Theorem 3 (Carbon Budget of the Macrocycle Core)**.** *Let one chrysene unit (18 carbon atoms) undergo rearrangement while its four attached substituents are retained, in whole or in part, as the metal-coordinating arms. Each substituent contributes at most 4 carbon atoms that can survive the rearrangement. Then the resulting metal-coordinated core contains between 26 and 34 carbon atoms.*

Proof. Write C_{core} for the number of carbon atoms in the final metal-coordinated macrocycle. The first chrysene supplies a fixed contribution of 18 atoms. Let k_i ($i = 1, 2, 3, 4$) be the number of carbon atoms retained from the i-th substituent arm; the chemical constraints of the linker geometry imply

$$0 \le k_i \le 4.$$

Hence

$$C_{\text{core}} = 18 + \sum_{i=1}^{4} k_i$$

and the possible values of the sum range from 0 to 16. The chemically realistic regime after minimal loss of linker atoms (at least two carbons retained per arm on average) restricts the sum to the interval $[8, 16]$. Consequently

$$C_{\text{core}} \in \{26, 27, \ldots, 34\}.$$

In particular the observed geological window C_{28}–C_{34} is contained in the predicted interval. □

Remark 4. *The argument is purely combinatorial and depends only on the carbon count of chrysene and on the maximal carbon content of each of the four arms. No assumption about the detailed bond-reorganisation trajectory is required.*

3.5 Fate of the Second Chrysene

Definition 4 (Step-Defect Linearisation)**.** *Controlled scission of the outer bonds of the second chrysene unit converts the fused tetracyclic system into a continuous linear chain of eighteen carbon atoms. The original step-defect geometry leaves four carbons of this chain in positions that correspond to the characteristic methylation sites of the interior segment of a β-carotene-type isoprenoid.*

Proposition 4 (Isoprenoid Scaffold)**.** *The linear* C_{18} *chain of Definition 4, once methylated at the four step-defect carbons, constitutes a geometric scaffold for a phytol-like isoprenoid tail. In the geological record the long tail is lost early; only the metal-coordinated core of Proposition* **??** *survives.*

Theorem 5 (Linearisation to a β-Carotene-Type Branching Pattern)**.** *Let G be the molecular graph of a* $3, 6, 9, 12$*-tetrasubstituted chrysene. Perform the following bond scissions:*

1. *the central fusion bonds* C4a–C4b *or* C10a–C10b*, and*
2. *the additional ring-closure bonds* C12a–C4a*,* C10b–C4b *and* C10a–C6b

(so that every fused ring is opened). The resulting graph is a single linear path P on the original eighteen carbon atoms of the chrysene core. Moreover, the four vertices that originally carried the substituents at positions $3, 6, 9, 12$ *appear on P at mutual distances that realise the alternating spacing pattern*

$$\begin{aligned}&\text{–C–C–C}^{*}\text{–C–C–C–C}^{*}\text{–C–C–}\\&\text{C–C–C}^{*}\text{–C–C–C–C}^{*}\text{–C–C–}\end{aligned}$$

where each C^{*} *denotes a carbon that was a substitution site. This is precisely the relative positioning of the four interior methyl-branching carbons in the central region of a β-carotene-type isoprenoid.*

Proof. Chrysene consists of four fused benzene rings whose carbon skeleton may be regarded as an 18-vertex planar graph. The bonds listed in the statement are exactly the edges whose removal destroys every cycle and leaves a spanning path: each scission increases the number of connected components of the cycle space by one, and after the complete set of scissions the cycle space is trivial. Hence the surviving graph is a tree; because the original graph is 2-connected and the removed edges are bridges of the dual, the tree is in fact a path P of length 17 (eighteen vertices).

It remains only to locate the original substitution vertices on P. In the standard numbering of chrysene the positions $3, 6, 9, 12$ lie on the outer perimeter and are separated by three intervening carbon atoms along that perimeter. When the fused system is opened into a Hamiltonian path that follows the perimeter (the unique path compatible with the chosen scissions), those four vertices remain separated by the same

three-carbon intervals. Consequently they appear on P in the exact sequential pattern

$$\ldots\text{–C–C–C}^{*}\text{–C–C–C–C}^{*}\text{–C–C–}$$
$$\text{C–C–C}^{*}\text{–C–C–C–C}^{*}\text{–C–C–}\ldots$$

which is the combinatorial signature of the four interior methyl-branching sites of a β-carotene-type isoprenoid chain.
The argument uses only the adjacency relation of the chrysene graph and the choice of scission set; no metric embedding or energetic hypothesis is required. □

Remark 5. *The four* C^{*} *carbons are therefore geometrically pre-organised for methylation. Any subsequent enzymatic (or abiotic) methyl-transfer step that acts on these sites converts the linear* C_{18} *chain into a methyl-branched isoprenoid scaffold without further spatial instruction from the enzyme. This supplies the precise link between the step-defect geometry of the opened chrysene and the characteristic branching pattern of the phytol-like tail.*

3.6 Transitional Phosphorus-to-Nitrogen Coordination

Proposition 6 (Ligand Evolution)**.** *The four phosphorus-centred linkers of Definition 3 are chemically competent to hold the metal ion. Replacement or evolutionary transformation of these linkers into nitrogen-bearing ligands yields the classic* N_4 *coordination sphere of biological chlorophyll and of the geological Ni- and VO-porphyrins, while preserving the metal-binding geometry of the cage.*

Remark 6. *Phosphorus therefore functions as a transitional coordinating element. Its presence in the initial cage is consistent with the broader metal–phosphorus integration theme of the Chrysene Formalism; its absence from the final geoporphyrins is the expected outcome of ligand evolution.*

3.7 UV-Driven Lattice Melting and Rearrangement Protocol

We record a chemically explicit, stepwise sequence by which a dual-chrysene metal cage embedded in a π-stacked aromatic lattice can undergo photochemically initiated reorganisation into a metal-coordinated tetrapyrrole. The sequence is offered as a geometric-chemical hypothesis consistent with the definitions of Section 3; it is not claimed as an experimentally verified laboratory protocol.

Definition 5 (Natural Photochemical Setting)**.** *The dual-chrysene metal cage of Definition 3 is situated within a larger* π*-stacked assembly of chrysene-derived aromatic units. The four substituents that close the cage occupy the* $3, 6, 9, 12$*-type positions of each chrysene and are of the phosphorus-centred linker type*

$$\text{–O–CH}_2\text{CH}_2\text{–OPO}_2\text{O–CH}_2\text{CH}_2\text{–O–}.$$

A metal ion is already coordinated inside the cage. The entire assembly is exposed to near-ultraviolet radiation that is absorbed both by the chrysene chromophores and, to a lesser extent, by the metal centre.

Protocol 1 (Stepwise Rearrangement)**.** *The following sequence is proposed:*

1. ***Photon absorption and local excitation.*** *A near-UV photon is absorbed by one of the two cage chrysenes (or by an adjacent unit in the* π*-stack). The resulting* S_1 *or higher excited state is rapidly localised on the first chrysene unit (the unit destined to become the macrocycle).*
2. ***Transient weakening of aromatic stabilisation.*** *Excitation reduces the local aromatic stabilisation energy of the first chrysene, effectively "melting" the rigidity of selected peripheral bonds while the metal ion and the four linkers remain in place. This step corresponds to the lattice-melting event of the Formalism.*
3. ***Selective carbon–carbon bond scission.*** *Under the steric constraint imposed by the four tethered substituents, two (or more) peripheral C–C bonds of the first chrysene undergo scission. The geometry of the* $3, 6, 9, 12$*-substitution pattern directs the scission so that the resulting fragments remain covalently attached to the phosphorus-centred linkers.*
4. ***Reorganisation around the metal centre.*** *The partially opened first chrysene, still held by the four linkers, re-closes around the metal ion. In the course of re-closure the original fused-ring topology is converted into a tetrapyrrole-like macrocycle. Nitrogen atoms are either unmasked from the original lattice or introduced by exchange with the phosphorus-centred linkers (Proposition 6), yielding the classic* N_4 *coordination sphere.*
5. ***Concurrent linearisation of the second chrysene.*** *Simultaneously, or immediately thereafter, the second chrysene unit undergoes controlled scission of its outer bonds (Definition 4). The product is a linear* C_{18} *chain whose step-defect carbons occupy positions suitable*

for subsequent methylation, thereby generating the geometric precursor of the phytol-like tail.

6. ***Relaxation and aromatisation.*** *The newly formed metal-coordinated macrocycle relaxes into a fully conjugated* $18\,\pi$*-electron system (Proposition* **??***). Any residual strain is relieved by the same thermal or photochemical energy that initiated the sequence. The linear tail remains attached only loosely and is subsequently lost under diagenetic conditions (Proposition 10).*

Remark 7 (Chemical Plausibility)**.** *The sequence relies on three well-documented photochemical motifs:*

- *near-UV absorption by polycyclic aromatic hydrocarbons,*
- *excited-state bond weakening and selective scission in constrained aromatic systems,*
- *metal-templated macrocyclisation.*

The four $3, 6, 9, 12$*-type tethers supply the steric preorganisation that makes the re-closure around the metal geometrically favoured over indiscriminate fragmentation. Phosphorus-to-nitrogen ligand exchange is chemically precedented in coordination chemistry and is consistent with the transitional role assigned to phosphorus in Proposition 6.*

Remark 8 (Carbon and Electron Accounting)**.** *Throughout the protocol the* $18\,\pi$*-electron count is conserved, and the carbon atoms of the first chrysene plus the retained portions of the four arms remain inside the* C_{26}–C_{34} *window fixed by Proposition* **??***. No external carbon source is required.*

4 Consistency with the 1.1 Ga and Related Records

The geometric constructions of Section 3 are now confronted with the observational constraints fixed in Section 2. Each subsection records a distinct consistency; none is advanced as a uniqueness proof.

4.1 Carbon-Number Match

Proposition 7 (Carbon-Number Consistency)**.** *The metal-coordinated core generated by Proposition* **??** *occupies the carbon-number interval* C_{26}–C_{34}*. The dominant geoporphyrins of the* 1.1 Ga *Taoudeni Basin assemblage occupy the sub-interval* C_{28}–C_{34}*. The predicted interval therefore contains the observed distribution.*

Remark 9. *The modest extension of the predicted window to* C_{26} *is a geometric upper bound on carbon loss from the substituent arms; it does not contradict the empirical concentration at* C_{28}–C_{34}*.*

4.2 Structural-Class Match

Proposition 8 (DPEP and Etio Trajectories)**.** *The bond-reorganisation pathways open to the first chrysene unit under lattice melting include both:*

1. *trajectories that retain a five-membered exocyclic ring, yielding a DPEP-type macrocycle, and*
2. *trajectories that open or omit that ring, yielding an Etio-type macrocycle.*

Both structural classes are present in the 1.1 Ga *record, and the maturity-dependent conversion DPEP → Etio observed throughout the sedimentary column is consistent with progressive opening of the exocyclic ring under thermal stress.*

4.3 Metal-Identity Match

Proposition 9 (Metal Agnosticism of the Cage)**.** *At the purely geometric level the dual-chrysene cage of Definition 3 imposes no restriction on the identity of the coordinated metal ion. The metals that dominate the geological record—nickel(II) and vanadyl (*VO^{2+}*)—are precisely those that survive diagenetic exchange and reduction. The geometric model is therefore compatible with the observed metal distribution; it does not predict, nor does it contradict, the preference for Ni and VO over other transition metals.*

4.4 Tail Loss

Proposition 10 (Lability of the Linear Chain)**.** *The linear* C_{18} *(or* C_{18+}*) chain generated by Definition 4 is aliphatic and non-aromatic. Relative to the fully conjugated, metal-coordinated core it is therefore expected to be the more labile moiety under diagenetic conditions. Its early and essentially universal loss from the geological record is the predicted outcome; only the aromatic core of Proposition* **??** *survives.*

Remark 10. *Collectively, Propositions 7–10 establish that the principal empirical regularities of the* 1.1 Ga *and younger geoporphyrin records—carbon-number window, coexistence of DPEP and Etio classes, metal identities, and early tail loss—lie inside the geometric envelopes fixed by*

the dual-chrysene cage. Finer isomer-specific or atomistic tests remain beyond present resolution and constitute open experimental targets.

4.5 Pre-organisation, Metal Insertion, and the Role of the Surrounding π-Stack

The dual-chrysene metal cage of Definition 3 is not assumed to form spontaneously. We record a geometrically directed sequence by which free tetrasubstituted chrysene units and a divalent metal ion assemble into the closed cage, and by which the surrounding π-stack both assists metal entry and subsequently channels the photochemical energy required for rearrangement.

Definition 6 (Pre-organised Cavity)**.** *Two tetrasubstituted chrysene units of native C_{2h} symmetry, oriented face-to-face, generate a discrete interstitial cavity whose dimensions are fixed by the lengths of the four* 3, 6, 9, 12*-type substituents. When the substituents are of the phosphorus-centred linker type, the cavity presents an electrostatic and steric profile complementary to a divalent metal ion.*

Proposition 11 (Directed Metal Insertion)**.** *Metal insertion into the cavity of Definition 6 proceeds under geometric control:*

1. *the four substituents act as pre-organised ligands that lower the entropic barrier to coordination;*
2. *one side of the pair remains transiently open, permitting metal entry;*
3. *once the metal ion is coordinated, the open side may close (or remain only partially open), locking the ion inside the cage.*

No external template is required; the substitution geometry of the chrysene lattice itself supplies the necessary pre-organisation.

Definition 7 (Surrounding π-Stack)**.** *The dual-chrysene cage is embedded in a larger assembly of π-stacked chrysene-derived aromatic units. At least two additional stacked layers (one on each face of the cage pair) are assumed.*

Proposition 12 (Dual Role of the π-Stack)**.** *The surrounding π-stack performs two distinct geometric functions:*

1. ***Steric clamp.*** *The additional stacked units restrict the conformational freedom of the four linkers, thereby favouring productive closure around the metal over dissociation or indiscriminate oligomerisation.*
2. ***Energy funnel.*** *The extended aromatic assembly absorbs near-ultraviolet photons and can transfer excitation energy to the cage pair, increasing the effective cross-section for the lattice-melting step of Protocol 1.*

Corollary 1 (Assembly Sequence)**.** *The geometrically natural order of events is therefore:*

1. *face-to-face association of two tetrasubstituted chrysenes, forming the pre-organised cavity;*
2. *insertion of a divalent metal ion;*
3. *locking of the cage by linker closure or by the steric pressure of the surrounding π-stack;*
4. *subsequent photochemical rearrangement of the locked cage according to Protocol 1.*

Remark 11. *The sequence remains carbon-parsimonious and closed: every carbon atom that appears in the final metal-coordinated macrocycle or in the linear tail precursor is already present in the two chrysene units and their four substituents. The surrounding π-stack functions only as a steric and photochemical auxiliary; it need not contribute carbon atoms to the product.*

Proposition 13 (Symmetry Reduction and Local Restoration)**.** *The dual-chrysene metal cage begins with two units of global symmetry C_{2h}. Under the rearrangement of Protocol 1 the following symmetry sequence occurs:*

1. *the face-to-face pair and the subsequent bond scissions break the original C_{2h} symmetry of each individual chrysene;*
2. *Re-closure of the four substituent arms about a single metal centre restores a local four-fold rotational approximate symmetry, so that the immediate coordination environment of the metal approaches the idealised point-group D_{4h} of a metalloporphyrin, while the peripheral substituents keep the global molecular symmetry strictly lower.*
3. *the peripheral alkyl substituents and any residual asymmetry of the macrocycle keep the global molecular symmetry strictly lower than D_{4h}.*

Thus the passage from the dual-chrysene cage to the metal-coordinated core is a symmetry-breaking / local-symmetry-restoration sequence.

Remark 12 (Representation-theoretic reading)**.** *The local four-fold rotational approximate symmetry (approaching the idealised coordination environment of a metalloporphyrin while the peripheral substituents keep the global molecular symmetry strictly lower). The leading electrostatic multipoles of this representation coincide with those of the biological* N_4 *coordination sphere. Consequently any enzymatic surface that recognises the local four-fold electrostatic pattern of the geometric product can bind the later biosynthetic copies without further redesign of the recognition domain. This supplies the precise link between the geometric model and the "electrostatic and symmetry adaptation" claim of the enzymatic-consistency section.*

4.6 Extension to Heme: A Geometric Corollary

The metal-coordinated macrocycle generated by the dual-chrysene rearrangement is not restricted to the magnesium-containing chlorin series of chlorophyll. The same geometric product is compatible with the iron-containing tetrapyrrole of heme. We record this compatibility as a formal corollary.

Corollary 2 (Geometric Origin of the Heme Macrocycle)**.** *The dual-chrysene metal cage of Definition 3, under the rearrangement of Protocol 1, yields a metal-coordinated* $18\,\pi$*-electron tetrapyrrole whose carbon-number window, four-arm coordination geometry and aromatic pathway are identical to those required by heme (Fe-protoporphyrin IX and its geochemical derivatives). Consequently the Chrysene Formalism supplies a common geometric precursor for both the photosynthetic (chlorophyll-type) and the respiratory / redox (heme-type) macrocycles.*

Proof. Heme consists of an $18\,\pi$-electron porphyrin macrocycle coordinated to a central iron ion by four nitrogen atoms, with a carbon skeleton that, after the usual diagenetic defunctionalisation, falls inside the same C_{26}–C_{34} interval already established for the geoporphyrins (Theorem 3). The rearrangement of Protocol 1 produces precisely such a macrocycle; the only variable that distinguishes a chlorophyll-type product from a heme-type product is the identity of the metal ion that occupies the central cavity (Mg versus Fe) and the precise peripheral substitution pattern. Because the dual-chrysene cage is metal-agnostic at the geometric level (Proposition 9), both metals are admissible. The $18\,\pi$-electron invariance (Theorem 2) is likewise independent of the metal. Therefore every structural invariant required by heme is already realised by the geometric product of the dual-chrysene cage. □

Remark 13 (Photochromic Parallel)**.** *Both chrysene and heme are photochromic: each possesses a conjugated* π*-system that undergoes well-defined electronic excitation and subsequent structural or redox response upon absorption of light. In the present framework the photochromicity of the parent chrysene lattice is the physical agent that initiates lattice melting; the photochromicity of the resulting heme (or chlorophyll) macrocycle is the evolutionary continuation of the same electronic motif. The Formalism therefore links the light-driven formation of the macrocycle to the light-responsive behaviour of the mature biological cofactor through a single, continuous* π*-electron system.*

Remark 14 (Geochemical Consequence)**.** *Etio-type geoporphyrins, which dominate many mature sedimentary assemblages, can arise either by thermal opening of a DPEP (chlorophyll-derived) precursor or by direct diagenetic alteration of a heme-type tetrapyrrole. The dual-chrysene pathway is compatible with both routes: the same geometric core can be realised with magnesium (leading, after diagenesis, to DPEP/Etio mixtures of chlorophyll provenance) or with iron (leading to Etio-type porphyrins of heme provenance). The model therefore does not force a unique biological source for every Etio geoporphyrin; it only asserts that both sources share a common geometric ancestor in the dual-chrysene cage.*

5 Consistency with Enzymatic Porphyrin Formation

The geometric rearrangement of the dual-chrysene metal cage supplies a concrete molecular prototype. Biological systems, however, do not rely on a one-time photochemical event; they require a reproducible enzymatic pathway. We record here the sense in which the geometric process is consistent with the subsequent emergence of such a pathway, while leaving the detailed nucleation of specific enzymes (ghost-pocket templating, negative-space catalysis, etc.) for later work.

5.1 The Geometric Prototype as Mastering Pattern

Definition 8 (Mastering Pattern)**.** *The metal-coordinated macrocycle together with its associated linear* C_{18} *chain, once formed by Protocol 1, constitutes a mastering pattern: a positive-space object whose shape, electrostatic profile and* $18\,\pi$*-electron aromaticity can be read by a complementary (negative-space) macromolecular surface.*

Proposition 14 (Negative-Space Complement)**.** *Any enzymatic surface that evolves to bind the mastering pattern of*

Definition 8 necessarily carries a complementary cavity. That cavity is the negative-space imprint of the porphyrin-like core and of the linear tail scaffold. Once the imprint exists, the same surface can catalyse the assembly of a new positive-space copy from simpler precursors, thereby converting a one-time geometric event into a repeatable biosynthetic cycle.

5.2 Isoprenoid Scaffold and Enzymatic Methylation

The linear C_{18} chain generated by opening of the second chrysene (Definition 4) already positions four carbons at the relative spacings characteristic of the interior methyl-branching pattern of a β-carotene-type isoprenoid.

Proposition 15 (Pre-organised Methylation Sites)**.** *The step-defect carbons of the linear chain constitute a geometric scaffold on which enzymatic methylation can operate with minimal additional spatial instruction. The resulting methyl-branched chain is then available for the further chain-elongation and cyclisation steps that produce the mature phytol (or related isoprenoid) tail of chlorophyll. Thus the geometric opening of the second chrysene supplies not only carbon atoms but also a spatial pre-pattern that later isoprenoid enzymes can exploit.*

5.3 Electrostatic and Symmetry Adaptation

Proposition 16 (Symmetry and Electrostatic Continuity)**.** *The dual-chrysene cage begins with two C_{2h} units. After rearrangement the metal-coordinated core approaches the higher idealised symmetry of a metalloporphyrin (locally approximating D_{4h} in the absence of peripheral substitution). The four nitrogen (or transitional phosphorus) ligands maintain a conserved electrostatic pattern—four partially negative coordination sites surrounding a central cation—that is identical in its leading multipole moments to the coordination sphere of modern chlorophyll and of the geological Ni- and VO-porphyrins. Any enzymatic pocket that recognises this electrostatic and symmetry signature can therefore bind both the original geometric product and its later biosynthetic copies without further redesign of the recognition surface.*

5.4 π-Electron Mapping

The 18 π-electron aromatic pathway is conserved throughout (Proposition **??**). Consequently the electronic absorption profile, the redox properties of the macrocycle, and the principal orbital symmetries remain recognisable to any enzyme that has evolved to interact with the mastering pattern. The π-electron count itself functions as an invariant that links the purely geometric precursor to the mature enzymatic product.

5.5 Summary of the Consistency Claim

The dual-chrysene rearrangement does not itself constitute the enzymatic pathway. It does, however, generate a mastering pattern whose

1. carbon-number window,
2. 18 π-electron aromaticity,
3. four-arm metal-coordination geometry,
4. linear isoprenoid-like scaffold, and
5. electrostatic and local-symmetry signature

are precisely the features that a subsequent enzymatic system must recognise and reproduce. In this limited but precise sense the geometric process is consistent with the later emergence of enzymatic porphyrin (and chlorophyll) biosynthesis: the positive-space object appears first; the negative-space enzymatic imprint can then form around it; thereafter the enzymes can replicate the positive space indefinitely.

Detailed mechanisms by which interstitial voids or ghost pockets might nucleate the first complementary enzymatic surfaces lie outside the scope of the present paper and are reserved for subsequent work.

Remark 15 (Scope of the Consistency Claim)**.** *The mastering-pattern and negative-space arguments of this section are offered solely as geometric consistency: they show that the dual-chrysene product possesses the structural, electronic and spatial features that a subsequent enzymatic system would need to recognise and reproduce. They do not assert a historical sequence of enzyme evolution, nor do they claim that the geometric prototype necessarily preceded the first biological catalysts in time.*

6 Testable Predictions and Open Questions

The geometric model of Section 3 generates a finite set of empirical consequences that can be confronted with existing or near-term analytical data. Each prediction is stated as a formal claim; the corresponding open problems are recorded immediately thereafter.

6.1 Carbon-Number and Isomer Patterns

Prediction 1 (Diagnostic Alkylation)**.** *If the metal-coordinated core derives from a chrysene unit plus four substituent arms, then the peripheral alkylation pattern of the resulting geoporphyrin should retain statistical traces of the original bridge lengths and substitution loci (in particular the* $3, 6, 9, 12$*- and related patterns). Isomer-specific or position-specific alkyl distributions that deviate from purely random side-chain attachment would constitute positive evidence for a chrysene-derived precursor.*

6.2 Step-Defect Methylation Scaffold

Prediction 2 (Pre-Positioned Methylation Sites)**.** *The linear* C_{18} *chain of Definition 4 carries four carbons whose relative spacing is fixed by the step-defect geometry of the parent chrysene. Enzymatic or abiotic methylation at precisely these sites is predicted to be geometrically preferred, thereby generating the characteristic opposing or* $1, 5$*-type methyl branching of the interior segment of a* β*-carotene-type isoprenoid. Any residual methylation pattern in immature tetrapyrrole-associated aliphatic fractions that matches this spacing would support the scaffold claim.*

6.3 Phosphorus as a Transitional Element

Prediction 3 (Residual Phosphorus)**.** *Because the initial metal-coordinating arms are phosphorus-centred, the most immature kerogen-bound tetrapyrrole fractions may retain trace phosphorus in spatial or chemical association with the aromatic core. Detection of such residual phosphorus—currently below routine analytical thresholds—would constitute direct evidence for the transitional ligand stage of Proposition 6.*

6.4 UV-Driven Rearrangement

Prediction 4 (Photochemical Competence)**.** *The dual-chrysene cage absorbs in the near-ultraviolet. Laboratory or high-level computational examination of whether absorption in this window can initiate the bond reorganisations required by Propositions* **??** *and 4 is therefore a well-posed experimental test of the melting step.*

6.5 Open Problems

The following questions lie beyond the present geometric resolution and define the frontier for subsequent work:

1. the detailed atomistic trajectory of the lattice melting and subsequent bond reorganisation that converts the first chrysene unit into the tetrapyrrole macrocycle;
2. the precise timing and chemical mechanism of the phosphorus-to-nitrogen ligand exchange;
3. whether any higher-carbon geoporphyrins ($> C_{34}$) retain detectable structural or isotopic signatures of the second chrysene unit before its complete conversion into the linear tail or its loss.

These open problems do not weaken the consistencies already established; they delimit the next empirical and computational targets required to move from geometric compatibility to atomistic verification.

7 Conclusion

The dual-chrysene metal-caged construct, once equipped with the carbon-partitioning rule of Proposition **??** and the step-defect linearisation of Definition 4, converts the 1.1 Ga geoporphyrin record from an independent biological fact into a geometric prediction of the Chrysene Formalism.

One chrysene unit, together with its four substituent arms, rearranges into an $18\,\pi$-electron, metal-coordinated macrocycle whose carbon numbers fall inside the observed C_{28}–C_{34} window. The second chrysene opens into a linear C_{18} chain whose step-defect carbons are pre-positioned for isoprenoid-type methylation, thereby supplying the geometric precursor of the phytol-like tail. Phosphorus-centred linkers hold the metal in the initial cage and are competent to evolve into the N_4 coordination sphere of chlorophyll and of the geological Ni- and VO-porphyrins.

The same architecture that, in earlier work, accounts for the co-production of membrane lipids and nucleic-acid components therefore also accounts for the core structural features of the photosynthetic macrocycle. The pre-Cambrian sedimentary archive consequently contains a second, independent geometric fossil of the metamaterial—complementary to the hopane/sterane asymmetry and to the macromolecular aromatic networks of kerogen already examined.

While atomistic trajectories and residual phosphorus signatures remain open experimental targets, the principal empirical regularities of the 1.1 Ga record already lie inside the geometric envelopes fixed by the dual-chrysene cage.

A Literature Review: Geoporphyrins, Chlorophyll Structure, and the 1.1 Ga Record

The empirical foundation of the present work rests on a substantial body of analytical studies of sedimentary porphyrins

and of the structure of biological chlorophyll. The following summary records the principal observational constraints that any geometric model of a photosynthetic-macrocycle precursor must respect.

A.1 Oldest Secure Geoporphyrins

Intact nickel and vanadyl geoporphyrins have been recovered from marine black shales of the Taoudeni Basin (Mauritania) dated at approximately 1.1 Ga [GMO+18]. The dominant species belong to the Etio and DPEP structural classes and occupy the carbon-number interval C_{28}–C_{34}. Nitrogen-isotope values of the purified porphyrins are consistent with a predominantly cyanobacterial source. This assemblage currently constitutes the oldest widely accepted molecular evidence of chlorophyll-derived pigments.

A.2 Structural Classes and Diagenetic Trends

Sedimentary porphyrins fall principally into two structural series: deoxophylloerythroetioporphyrin (DPEP), which retains a five-membered exocyclic ring, and etioporphyrin (Etio), which lacks that ring [Tre36, DAPE75, CO00]. With increasing thermal maturity the relative abundance of DPEP declines while that of Etio rises, indicating progressive opening or loss of the exocyclic ring [DAPE75, HOB96]. The long phytol side-chain of biological chlorophyll is lost early; only the metal-coordinated tetrapyrrole core together with short alkyl substituents survives into the geological record [KPM90, CO00].

A.3 Metal Preferences

In virtually all ancient sediments the porphyrins occur as nickel(II) or vanadyl (VO^{2+}) complexes [FVB87, CO00]. Free-base or other metal complexes are rare. The preference for Ni and VO is a diagenetic feature; the original biological metal (magnesium in chlorophyll) is exchanged during early burial.

A.4 Modern Chlorophyll Benchmarks

Chlorophyll *a* is a C_{55} molecule whose structure comprises an 18 π-electron chlorin macrocycle, a central magnesium ion coordinated by four nitrogen atoms, and a C_{20} phytol tail esterified at the propionic-acid side-chain of ring D [Sch91, SRL+14]. The 18 π-electron aromatic pathway is a defining electronic feature of both chlorophylls and the geoporphyrins derived from them. After diagenetic demetallation, loss of the phytol tail and limited peripheral defunctionalisation, the surviving carbon skeleton falls naturally into the C_{28}–C_{34} window documented at 1.1 Ga.

A.5 Symmetry and Coordination

Free-base porphyrins approximate D_{2h} symmetry; insertion of a central metal raises the idealised local symmetry toward D_{4h} [Gou61]. Peripheral substituents and, in the case of chlorins, reduction of one pyrrole ring lower the global symmetry, yet the four-fold coordination environment of the metal remains the dominant electrostatic and geometric signature recognised by both biosynthetic enzymes and diagenetic metal-exchange processes.

A.6 Summary of Empirical Boundary Conditions

Collectively the literature establishes that:

1. the oldest secure geoporphyrins are C_{28}–C_{34} Ni- and VO-complexes of the Etio and DPEP series;
2. the phytol tail is lost early while the 18 π-electron aromatic core persists;
3. maturity drives a progressive conversion of DPEP to Etio;
4. the modern chlorophyll template supplies an 18 π-electron macrocycle, a four-arm metal-coordination geometry, and a linear isoprenoid tail.

These observables constitute the experimental boundary conditions against which the geometric predictions of the dual-chrysene cage are tested in the main text.

B A Lattice-Preserving Rearrangement Operator on the Chrysene Tensor Space

We work throughout in the pure-mathematical setting of the Chrysene Tensor Space $\mathcal{I}_C$. The constructions below are independent of any particular physical realisation; they supply the abstract operator whose image under the realisation map Φ is the dual-chrysene rearrangement of the main text.

B.1 Preliminaries

Definition 9 (Local Chrysene Component)**.** *An elementary component $c \in \mathcal{I}_C$ is a C_{2h}-symmetric aromatic core equipped with four distinguished substitution loci (the abstract counterparts of the* 3, 6, 9, 12*-positions) and with a π-stacking adjacency relation to neighbouring components.*

Definition 10 (Dual-Cage Configuration)**.** *A dual-cage configuration is a pair (c_1, c_2) of elementary components together with a metal-coordination datum m such that the four substitution loci of each component jointly stabilise m. The surrounding π-stacking relations of c_1 and c_2 with the remainder of the lattice are part of the configuration data.*

B.2 The Rearrangement Operator

Definition 11 (Lattice-Preserving Rearrangement Operator)**.** *The lattice-preserving rearrangement operator*

$$\mathcal{R} : \mathcal{I}_C \longrightarrow \mathcal{I}_C$$

acts on a dual-cage configuration $(c_1, c_2; m)$ *by the following rules:*

1. *$\mathcal{R}$ transforms the first component c_1 into a new core c_1' whose four substitution loci are re-oriented so that they form a stable four-fold coordination environment about the metal datum m;*
2. *$\mathcal{R}$ linearises the second component c_2 into a chain object c_2' (the abstract counterpart of the C_{18} step-defect chain);*
3. *$\mathcal{R}$ leaves invariant every π-stacking adjacency that does not involve the internal bonds of c_1 or c_2.*

In other words, $\mathcal{R}$ modifies only the chosen dual-cage pair and returns a configuration whose global π-stacking lattice is otherwise undisturbed.

B.3 Invariance and Early Error Correction

Theorem 17 (Preservation of the Ambient Lattice)**.** *Let $\Gamma \subset \mathcal{I}_C$ be any finite π-stacked assembly containing a dual-cage configuration $(c_1, c_2; m)$. Write $\Gamma' = \mathcal{R}(\Gamma)$ for the image of the assembly under the operator of Definition 11. Then:*

1. *the restriction of Γ' to the complement of $\{c_1, c_2\}$ is identical to the corresponding restriction of Γ;*
2. *every π-stacking adjacency that linked a component outside $\{c_1, c_2\}$ to the dual-cage pair is preserved (only the internal geometry of the pair is altered);*
3. *the metal datum m remains coordinated in Γ'.*

Consequently the global architecture of the lattice is stable under local rearrangement of any single dual-cage pair.

Proof. By clause (3) of Definition 11 the operator $\mathcal{R}$ is the identity on all components and all adjacency relations that do not belong to the chosen dual-cage pair. The only data that change are the internal bond structure of c_1 (re-oriented into a four-fold coordination environment) and the topology of c_2 (linearised). Both changes are confined to the interior of the pair; they do not delete or rewire any edge that connects the pair to the remainder of Γ. Hence the complement lattice is fixed, the external π-stacking relations survive, and the metal remains inside the newly formed coordination sphere. □

Corollary 3 (Early Error-Correction Property)**.** *The operator $\mathcal{R}$ realises a primitive form of structural error correction: a local defect or excitation that is confined to a single dual-cage pair can be resolved by rearrangement of that pair alone, without propagation of topological damage into the surrounding π-stacked lattice. The ambient aromatic architecture is thereby protected against local perturbation.*

Remark 16 (Relation to the Physical Realisation)**.** *Under the realisation map Φ the abstract operator $\mathcal{R}$ is sent to the concrete UV-driven rearrangement of Protocol 1. Theorem 17 then asserts that the conversion of one dual-chrysene metal cage into a porphyrin-like macrocycle (plus linear tail precursor) does not disturb the π-stacking of the neighbouring aromatic units—precisely the lattice-preserving property required for a robust, error-tolerant prebiotic architecture.*

C Relation to the Chrysene Formalism Corpus

The present work forms part of a continuing programme whose experimental starting point, pure-mathematical foundations and successive biological applications have been set out in earlier publications. We record here the precise dependence of the dual-chrysene cage rearrangement on that corpus.

C.1 Empirical Origin

The concrete molecular geometry from which the entire Formalism is abstracted is the demonstration that nucleic-acid sequences integrated within a phospholipid enclosure can be generated directly from a substituted chrysene precursor [Sch25]. That composition-of-matter result fixes the physical lattice whose discrete substitution pattern, π-stacking propensity and metal-coordination capacity are formalised in the present paper as the dual-chrysene metal cage.

C.2 Pure-Mathematical Framework

Two complementary volumes develop the underlying mathematics. The first constructs the discrete non-commutative state space, its cohomological invariants and the associated operator algebras [Sch26b]. The second supplies the tensorial and algebraic-geometric structure that governs maximal-entropy survival under topological strain [Sch26e]. The lattice-preserving rearrangement operator $\mathcal{R}$ of the preceding appendix is an instance of the general class of structure-preserving maps defined in those works; its invariance properties (Theorem 17) are direct consequences of the axioms of the Chrysene Tensor Space $\mathcal{I}_C$.

A further volume situates the same geometry within a broader algebraic account of the continuity of life [Sch26f]. The dual-chrysene cage and its rearrangement into an 18 π-electron metal-coordinated macrocycle are concrete realisations of the "geometric origins" programme developed there.

C.3 Metamaterial and Biological Realisations

Subsequent articles in the *Annals* apply the Formalism to successive layers of organisation. One examines the tetrasubstituted chrysene lattice as a programmable topological metamaterial capable of self-assembly and quantum-information encoding [Sch26d]. Another treats the dual-chrysene reactive volume as the source of the observed hopanoid–sterane asymmetry and of the transition from environmental to endogenous membrane scaffolds [Sch26a]. A third presents the claim that a single encodable topological metamaterial accounts for the origin, the intelligence architecture and the evolutionary trajectory of life [Sch26g].

Most recently, the macromolecular aromatic networks of pre-Cambrian kerogen have been interpreted as a geometric archive of the same lattice, preserving characteristic length scales, bridge chemistry and metal-integration motifs [Sch26c]. The present paper extends that archive from the insoluble kerogen matrix into the solvent-extractable geoporphyrin fraction, showing that the identical dual-chrysene geometry also supplies the carbon-number window, 18 π-electron aromaticity and four-arm coordination pattern of the oldest chlorophyll-derived (and heme-compatible) tetrapyrroles.

C.4 Position of the Present Work

Collectively these works establish a single geometric object—the tetrasubstituted chrysene lattice and its dual-cage metal configurations—whose successive images under the realisation map Φ account for:

1. the integrated synthesis of nucleic acid and phospholipid (the patent),
2. the hopane/sterane temporal asymmetry,
3. the macromolecular architecture of pre-Cambrian kerogen, and
4. the 1.1 Ga geoporphyrin record (the present paper).

The dual-chrysene cage rearrangement analysed here is therefore not an isolated hypothesis; it is the photosynthetic-macrocycle instance of a uniform geometric principle already shown to organise membrane, genetic and residual organic-matter archives across the pre-Cambrian.

References

[CO00] H. J. Callot and R. Ocampo. Geochemistry of porphyrins. In K. M. Kadish, K. M. Smith, and R. Guilard, editors, *The Porphyrin Handbook*, volume 1, pages 349–398. Academic Press, 2000.

[DAPE75] Borys M. Didyk, Yousif I. A. Alturki, Colin T. Pillinger, and Geoffrey Eglinton. Petroporphyrins as indicators of geothermal maturation. *Nature*, 256:563–565, 1975.

[FVB87] R. H. Filby and G. J. Van Berkel. Geochemistry of metal complexes in petroleum, source rocks and coals. In R. H. Filby and J. F. Branthaver, editors, *Metal Complexes in Fossil Fuels*, volume 344 of *ACS Symposium Series*, pages 2–39. American Chemical Society, 1987.

[GMO+18] N. Gueneli, A. M. McKenna, N. Ohkouchi, C. J. Boreham, J. Beghin, E. J. Javaux, and J. J. Brocks. 1.1-billion-year-old porphyrins establish a marine ecosystem dominated by bacterial primary producers. *Proceedings of the National Academy of Sciences*, 115:E6978–E6986, 2018.

[Gou61] Martin Gouterman. Spectra of porphyrins. *Journal of Molecular Spectroscopy*, 6:138–163, 1961.

[HOB96] B. Huseby, R. Ocampo, and C. Bauder. Porphyrin distributions and metal speciation in the Paris basin. *Organic Geochemistry*, 24:—, 1996. Representative maturity study.

[KPM90] B. J. Keely, W. G. Prowse, and J. R. Maxwell. The Treibs hypothesis: an evaluation based on structural studies. *Energy & Fuels*, 4:628–634, 1990.

[Sch91] Hugo Scheer. *Chlorophylls*. CRC Press, 1991.

[Sch25] Charles D. Schaper. Encoded design integrated synthesis of nucleic acids, and phospholipids, and related pharmaceutical products, 2025. Patent US 12,195,423.

[Sch26a] Charles D. Schaper. Differential catalyst geometries of the dual-chrysene metamaterial: Hopanoid–sterane asymmetry and the transition from environmental to endogenous supply annals of the chrysene formalism. *Annals of the Chrysene Formalism*, 1:196–208, 2026.

[Sch26b] Charles D. Schaper. *Foundations of the Chrysene Formalism: Cohomological Invariants, Operator Algebras, and the Discrete Noncommutative State Space*. Schaper Systems Press, San Francisco, CA, 2026. ISBN: 979-8-950371-08-0.

[Sch26c] Charles D. Schaper. Kerogen as a geometric archive of the chrysene formalism: Macromolecular aromatic networks, dimensional signatures, and metal integration in pre-cambrian shales. *Annals of the Chrysene Formalism*, 1:209–220, 2026.

[Sch26d] Charles D. Schaper. Programmable topological metamaterials: Self-assembly and quantum information encoding in the tetrasubstituted chrysene lattice. *Annals of the Chrysene Formalism*, 1:169–177, 2026.

[Sch26e] Charles D. Schaper. *Tensorial Framework of the Chrysene Formalism - Universal Algebraic Geometry and Maximal-Entropy Survival*. Schaper Systems Press, San Francisco, CA, 2026. ISBN: 979-8-950371-03-5.

[Sch26f] Charles D. Schaper. *The Geometric Origins and Continuity of Life: The Chrysene Formalism and the Algebraic Foundations of the Biosphere*. Schaper Systems Press, San Francisco, CA, 2026. ISBN: 979-8-950371- 02-8.

[Sch26g] Charles D. Schaper. The universal blueprint: One encodable topological metamaterial to explain the origin, intelligence, and evolution of life. *Annals of the Chrysene Formalism*, 1:178–195, 2026.

[SRL+14] Mathias O. Senge, Aoife A. Ryan, Keith A. Letchford, Stuart A. MacGowan, and Tamara Mielke. Chlorophylls, symmetry, chirality, and photosynthesis. *Symmetry*, 6:781–843, 2014.

[Tre36] Alfred Treibs. Chlorophyll- und häminderivate in organischen mineralstoffen. *Angewandte Chemie*, 49:682–686, 1936.